

# HORIZONTAL FLOW REGIMES IN FRACTURED MEDIA

G.J. WEIR

Industrial Research Ltd, PO Box 32-310, Lower Hutt, NZ

**SUMMARY** — Typical flow regimes occurring in a finite fractured reservoir, occupied by a single phase liquid, are discussed. Estimates are provided for the time at the beginning and end of each regime, and of the expected pressure drawdown within each regime. The evolution of flow regimes is problem dependent, and can vary with the fluid and rock parameters, the geometry of the reservoir and the fractures within it. Examples discussed and quantified include radial and linear flows, fracture flows, bilinear flows, parallel flows, block drawdown, and finite fracture regimes. Block flow parallel to the fractures is shown to be important at intermediate times.

## 1 INTRODUCTION

Withdrawing mass at a constant rate from a reservoir often produces distinctive flow regimes. These flow regimes often have an approximately self-similar (Burnell et al 1991) pressure reduction behaviour. For example, for early times, central withdrawal from a cylindrical reservoir produces circular flows, and the pressure decreases approximately logarithmically, as in the Theis solution (Earlougher 1977). The Theis solution is self-similar, with the argument depending only on the function  $r^2/t$ . For a bounded reservoir, and for long times, a new regime develops, in which pressure drawdown occurs essentially as if in a spatially constant reservoir.

To further illustrate the formation of approximate regime flows, we plot the pressure drawdown from a non-isotropic, fractured porous medium in Figure 1. The flow regimes are as shown in Figure 2. In the next section we show that the first regime is due to drawdown in the fractures; the second to bilinear flow; the third to block drawdown; and the final regime to whole reservoir drawdown.

In this idealised example, four regimes are apparent from Figure 1. Analysis of the Laplace Transform of pressure, given in the next section, shows that near the origin, the pressure decreases initially as  $t^{1/2}$ , then as  $t^{1/4}$ , later as  $t^{1/2}$ , and finally as  $t$ , where  $t$  is time. The corresponding pressure drawdown approximations of these regimes are shown as dotted lines in Figure 1, whereas the exact numerical result is shown as a solid line.

Useful information on the pressure drawdown is then available if the approximate time of the start and finish of a particular regime is known, and if the behaviour of pressure within the regime is known. A major aim of this paper is to enumerate the possible regimes which can develop in fractured media of finite extent.

Four Pressure Drawdown Regimes

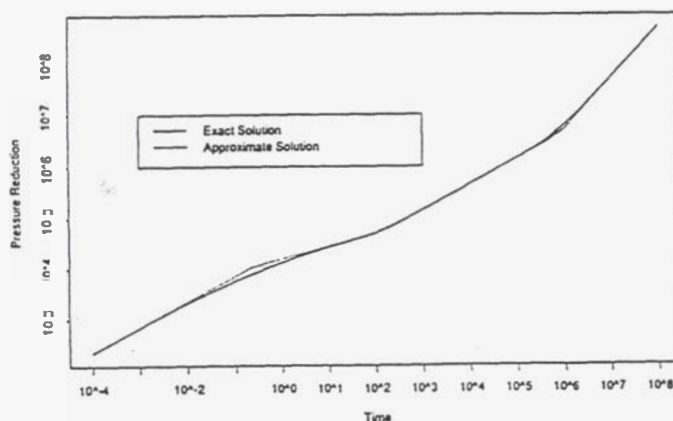


Figure 1. Analysis of flow in a finite fractured reservoir.

The physical motivation for this paper arises from the flow of hot water through a fractured porous media. This work is motivated by the need to understand system behaviour resulting from the flow of water in the lower regions of geothermal fields (Allis and Hunt, 1986), where pressures are sufficiently high to stop boiling, and where large and small scale fracturing of rock occurs widely.

The importance of preferential flow in porous media has been widely recognised for a considerable time. The analysis of radiation flows through a fissured media led to coupled diffusion equations - one in the media, and another in the fracture - yielding effectively the fracture block equations (Anzelius 1926 and Milne, 1926). Since these early papers, two main ideas concerning fractured porous media have developed.

The first idea considers the porous media to consist of a discrete number of blocks and fractures (alternatively fissures) so

that at each point in space, there is either a block or a fracture. We shall assume this model in this paper. The second idea considers the fractures to be so numerous that at each point in space there is simultaneously both a fracture and a block. This is the so-called double porosity model. Both ideas result in essentially identical equations.

Early developments in the petroleum industry lead to double porosity applications starting in the 1960's (Pollard 1959, Barenblatt et al 1960, Warren and Root 1963). Many field tests showed good agreement with these double porosity theories, and the resulting methods in well test interpretation have now become part of standard engineering practice (Earlougher 1977). The same methods have also been applied to geothermal applications (McGuinness 1986).

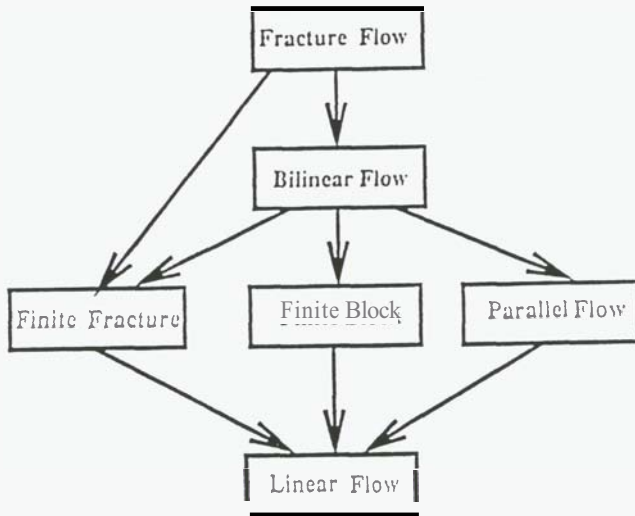


Figure 2. Flow regimes in a finite fractured reservoir.

Fully numerical models can treat some aspects of (multi-phase) flows through double porosity media. The most developed geothermal simulator treating double porosity media at present uses the **MINC** (multiple interacting continuum) code, developed by K Pruess (Pruess 1983). This code cannot model through-flow, in which a large fraction of the fluid flow occurs via the "uniform" media between the fractures. However, other code developed by Pruess (Pruess 1988) can approximate such effects, by considering a discrete system of fractures and blocks. For these reasons, it is important to understand the likely regimes which can occur, and to verify that the code can satisfactorily describe them.

The aim of this paper is to discuss factors determining the beginning and end of such regimes in more general examples, and to provide estimates for the corresponding pressure draw-down for each regime.

## 2 EQUATIONS

The equations describing liquid flow through a fractured porous medium can be simplified by assuming Darcy flow (Corey 1977) with constant fluid viscosity, compressibility and density, and ignoring gravity-work contributions. Denoting fracture and block parameters by subscripts of *f* and *b* respectively, the mass conservations equations are

$$\begin{aligned}\frac{\partial p_f}{\partial t} &= D_f (\nabla \cdot (\nabla p_f - \rho g) - \frac{k_b}{k_f \delta} \sum_{\alpha=1}^2 \nabla (p_b - \rho g) \cdot n^\alpha) \\ \frac{\partial p_b}{\partial t} &= D_b \nabla \cdot \nabla (p_b - \rho g)\end{aligned}\quad (1)$$

The diffusivities ( $D_f$  and  $D_b$ ) satisfy

$$D_f = \frac{k_f}{C \mu \phi_f} \quad (2a)$$

$$D_b = \frac{k_b}{C \mu \phi_b} \quad (2b)$$

The flow equations above can be nondimensionalised by introducing the definitions

$$p - \rho g = \frac{\mu Q}{\rho k_b} P \quad (3a)$$

$$t = \frac{k_f^2 \delta^2}{k_b^2 D_f} T \quad (3b)$$

$$x = \frac{\delta k_f}{k_b} X \quad (3c)$$

$$\epsilon = \frac{D_b}{D_f} \quad (3d)$$

where  $P, T, X$  are nondimensional pressures, time and positions. Equations (1) then simplify to

$$\frac{\partial P_f}{\partial T} = \nabla \cdot \nabla P_f - \sum_{\alpha=1}^2 \nabla P_b \cdot n^\alpha \quad (4a)$$

$$\frac{\partial P_b}{\partial T} = \epsilon \nabla \cdot \nabla P_b \quad (4b)$$

and in Cartesian geometries, the source boundary conditions is

$$\left. \frac{\partial P_f}{\partial X} \right|_0 = 1 \quad (5)$$

### 2.1 Laplace Transform Analysis of Anisotropic 'Block Flow

In this subsection we consider a fracture of length  $l$  and width  $b$ , surrounded by two blocks of length  $l$  and width  $w/2$ . Flow in the fracture is assumed to be only in the  $x$  direction, and only flow in the  $y$  direction is allowed in the blocks. We assume also that uniform conditions hold in the third dimension. The equations, initial and boundary conditions describing these assumptions are

$$\frac{\partial P_f}{\partial T} = \frac{\partial^2 P_f}{\partial X^2} + 2 \left. \frac{\partial P_b}{\partial Y} \right|_0 \quad (6a)$$

$$\frac{\partial P_b}{\partial T} = \epsilon \frac{\partial^2 P_b}{\partial Y^2} \quad (6b)$$

$$P_f = 0 = P_b \text{ at } T = 0 \quad (7)$$

$$\frac{\partial P_f}{\partial X} = 0 \text{ at } X = L \quad (8a)$$

$$\frac{\partial P_b}{\partial Y} = 0 \text{ at } Y = W/2 \quad (8b)$$

where the nondimensional distances  $L$  and  $W$  are defined as

$$L = \frac{k_b l}{k_f \delta} \quad (9a)$$

$$W = \frac{k_b w}{k_f \delta} \quad (9b)$$

Taking Laplace Transforms (Carslaw and Jaeger 1978) ,

$$\bar{P} = \int_0^\infty e^{-sT} P dT \quad (10)$$

yields the transformed solution

$$\alpha^2 = S + \frac{2\sqrt{\frac{s}{\epsilon}}(1 - e^{-\sqrt{\frac{s}{\epsilon}}W})}{(1 + e^{-\sqrt{\frac{s}{\epsilon}}W})} \quad (11a)$$

$$\bar{P}_f = -\frac{(e^{-\alpha X} + e^{-2\alpha L + \alpha X})}{\alpha S(1 - e^{-2\alpha L})} \quad (11b)$$

$$\bar{P}_b = \bar{P}_f \frac{(e^{\sqrt{\frac{s}{\epsilon}}(Y-W)} + e^{-\sqrt{\frac{s}{\epsilon}}Y})}{(1 + e^{-\sqrt{\frac{s}{\epsilon}}W})} \quad (11c)$$

The four different regimes can be understood from the different limiting forms of  $\alpha$ . At early times, or for large values of  $S$ ,  $\alpha \sim \sqrt{S}$ , representing the early fracture flow. The bilinear flows begin when  $S \sim 2\sqrt{(S/\epsilon)}$ , which suggests  $S \sim 4/\epsilon$ , or  $T \sim \epsilon/4$ . The corresponding dimensional time is

$$t = \left(\frac{\phi_f \delta}{\phi_b}\right)^2 \frac{1}{4D_b} \quad (12)$$

which is when flow from the block becomes important, relative to fracture flow. The finite width of the blocks becomes important when  $T \sim 1/S \sim W^2/\epsilon$ , or in dimensional form,  $t \sim w^2/D_b$ . Finally, at very long times, or for very small values of  $S$ ,  $\alpha^2 \sim (1 + W/\epsilon)S$ , and this approximation is expected to occur after about

$$t = \frac{4l^2}{D_f} \left(1 + \frac{w\phi_b}{\delta\phi_f}\right) \gg \frac{4l^2}{D_f} \quad (13)$$

A more rigorous derivation of the transition times above can be derived by analysing the pressure response at the origin. Putting  $X = 0$ , and  $\alpha = \sqrt{S}$  yields

$$p_f - \rho g z = -\frac{2\mu Q}{\rho k_f \delta} \sqrt{\frac{D_f t}{\pi}} \quad (14)$$

which is the approximate early behaviour for flow confined only to the fracture.

The following bilinear flow behaviour can be inferred by setting  $X = 0$ , and  $\alpha^2 = 2\sqrt{S/\epsilon}$ , yielding

$$p_f - \rho g z = -\frac{\mu Q (D_b t)^{\frac{1}{2}}}{\sqrt{2}\Gamma(\frac{3}{4})\rho} \sqrt{\frac{1}{k_b k_f \delta}} \quad (15)$$

which is the approximate behaviour for bilinear flow.

The two pressures in (14) and (15) are equal when

$$t \sim \left(\frac{\phi_f \delta}{\phi_b}\right)^2 \frac{1}{4.4D_b} \quad (16)$$

which is in good agreement with the estimate in (12). Since the time for bilinear flow to develop is based essentially on the square of fracture width divided by the block diffusivity, it is clear that bilinear flow will always occur before the finite width of the block is seen in the pressure response. It is possible that the finite length of the fracture may be seen before bilinear flow occurs, but this requires

$$\frac{l^2}{D_f} < \frac{\phi_f^2 \delta^2}{4\phi_b^2 D_b} \quad (17)$$

This inequality is unlikely to hold in many cases. For example, with a fracture length of 100 m, fracture width of 1 m, fracture and block porosities approximately equal, and fracture permeability 1000 times greater than block permeability! then the inequality in (17) does not hold. In such cases, bilinear flow will develop before the end of the fracture is seen.

For completeness, we show the regimes which result when the inequality in (17) holds. The corresponding graph is given in Figure 3, which shows slope doubling (rather than slope halving which occurs for bilinear flows) at the end of the initial fracture flow regime.

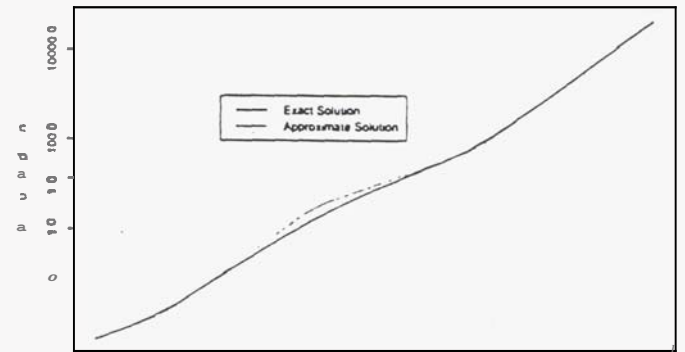


Figure 3. Example showing slope doubling.

The inequality in (17) can be expressed nondimensionally as

$$2L < \sqrt{\epsilon} \quad (18)$$

For  $2L < \sqrt{\epsilon}$ , the finite fracture regime develops; otherwise bilinear flow begins.

When the fracture length is large relative to block width, a third regime begins, when the finite block width begins to affect the pressure response. This occurs for small values of  $S$ , when the exponential terms containing  $W$  in (11a) can be expanded in a power series, yielding  $\alpha^2 \sim S(1 + W/\epsilon)$ , and so

$$p_f - \rho g z = -\frac{2\mu Q}{\rho k_f \delta} \frac{\delta \phi_f}{(\delta \phi_f + w \phi_b)} \sqrt{\frac{D_f t}{\pi}} \quad (19)$$

The time that this new regime begins is obtained by equating the pressures in (19) and (15),

$$t = \frac{4\pi^2}{\Gamma(\frac{1}{4})} \frac{\phi_f^2}{\phi_b^2} \frac{\delta^2}{D_b} \left(1 + \frac{w \phi_b}{\delta \phi_f}\right)^2 \quad (20)$$

which reduces to  $t \sim w^2/4/D_b$  when the block width is much greater than the fracture width.

The final regime is derived by assuming that both the finite block width and finite fracture length are affecting the pressure response. Then  $\alpha^2 = S(1 + W/\epsilon)$ , and

$$p_f - \rho g z = -\frac{Q t}{\rho l C (\delta \phi_f + w \phi_b)} \quad (21)$$

This final regime can be understood from a total mass balance. If  $b$  is the height of the reservoir, then at time  $t$ ,  $Qbt$  of mass has been withdrawn. The total volume of the reservoir is  $bl(\delta \phi_f + w \phi_b)$ . The ratio of the mass of water withdrawn to the total reservoir volume is approximately  $\rho C \Delta p$  where  $\Delta p$  is the average change in pressure. This is just the expression in (21).

Figure 1 shows that the four regimes analysed above are correct. Figure 1 was drawn assuming  $\epsilon = .1$ ,  $W = 5$ ,  $L = 100$ . The sequence of four regimes are quite clear, with successive slopes of .5, .25, .5, 1. The expressions in the subsection above have been used in constructing the approximate pressure drawdown, and the times for the beginning and end of each regime.

Figure 2 emphasises the non-unique development of the regimes. The sequence analysed in this subsection involve fracture flow, bilinear flow, finite block flow and linear flow. The sequence analysed in Appendix A involves fracture flow, finite fracture flow (comprising of slope doubling and then slope halving) followed by linear flow. The last section of this paper justifies the parallel flow regime shown in Figure 2.

## 2.2 Regime equations

Four flow regimes were identified above. We shall argue later that the third regime is unlikely to develop in nature. We

shall now state the three fundamental equations describing the first, second and final regimes above.

The first regime is simply fracture flow alone,

$$\frac{\partial P_f}{\partial T} = \nabla \cdot \nabla P_f \quad (22)$$

which admit similarity solutions with arguments of  $x^2/t$ . The initial regime then has a pressure drawdown with parameters corresponding to a homogeneous medium with magnitudes equal to those for the fracture system.

The bilinear regime develops when the flow from the block into the fracture system becomes important and before pressures propagate along the fracture system. In this case, the bilinear regime will occur, and the flow to the well results from a quasi-steady flow from the blocks alone. The approximate pressure fracture equation for this regime is

$$\nabla \cdot \nabla P_f = \sum_{\alpha=1}^2 \nabla P_b \cdot n^\alpha \quad (23)$$

and since time derivatives of fracture pressure are relatively unimportant in this regime, the gradients of block pressure at fracture boundaries will approximately satisfy

$$\nabla P_b \cdot n^\alpha \simeq \frac{P_f}{\sqrt{(\pi \epsilon T)}} \quad (24)$$

Consequently, the new (bilinear) regime can admit  $X^2/\sqrt{(\epsilon T)}$  as a self-similar variable.

The final regime, in which the block and fracture pressures drawdown approximately equally, follows from simple volumetric balances.

## 3 Parallel flow regime

It is clear that for early times, the dominant flow directions from the blocks to the fractures will be approximately normal to fracture surfaces. We show in this section that for late times it is likely that this flow pattern in the blocks will change to being parallel to the fracture surfaces. Similar conclusions have been reached by Kissling and Young (Kissling and Young 1989) and Young (Young 1992).

Our argument will only be developed close to the spatial origin, where both  $X$  and  $Y$  are assumed to be small. Near the sink, the pressure gradient in the fracture is essentially constant for constant production, since

$$\left. \frac{\partial P_f}{\partial X} \right|_0 = 1 \quad (25)$$

Such fracture pressure gradients will be transmitted to the blocks, because pressure is continuous, and so pressure gradients in the blocks parallel to the fractures are also continuous



at the fracture-block boundaries. This parallel pressure gradient will produce a flow in the blocks, but initially such flows are insignificant relative to the normal flows from the blocks to the fractures.

However, in the blocks, the pressure gradient normal to fractures decreases with time, whereas the parallel pressure gradients are essentially constant, at least close to the sink. Near the sink, and during the bilinear regime,

$$\left. \frac{\partial \bar{P}_b}{\partial Y} \right|_0 \sim \frac{1}{\sqrt{2\epsilon} \frac{1}{4} S^{\frac{1}{2}}} \quad (26)$$

and so

$$\left. \frac{\partial P_b}{\partial Y} \right|_0 \sim \frac{1}{\sqrt{2\epsilon} \frac{1}{4} \Gamma(\frac{3}{4}) T^{\frac{1}{4}}} \quad (27)$$

Once this normal block pressure gradient reduces to about unity, the parallel flows become important, and the parallel regime begins. This occurs when

$$T \sim \frac{1}{9\epsilon} \quad (28)$$

or in dimensional form,

$$t \sim \frac{k_f^2}{9k_b^2} \frac{\delta^2}{D_b} \quad (29)$$

We have assumed that the transition from bilinear to parallel flow occurs during the bilinear regime, and before the finite block size has affected pressures. The finite block size occurs after about  $t \sim w^2/D_b$ , and so we have assumed

$$\frac{w^2}{D_b} > \frac{k_f^2}{9k_b^2} \frac{\delta^2}{D_b} \quad (30)$$

which is equivalent to

$$3W > 1 \quad (31)$$

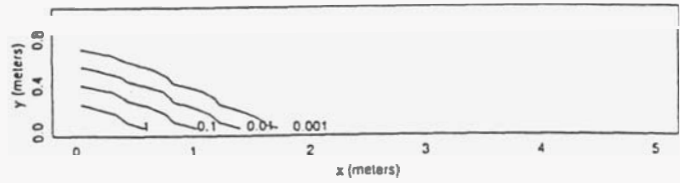
and so the nondimensional number  $W$  determines whether parallel flow begins before finite block effects.

The drawdown of pressure in the parallel regime depends critically on the dimensionality of the flow at the origin. Since steady flows are possible in three dimensions, the pressure can be approximately constant at the origin during the parallel flow regime (Young 1992). The two dimensional flows in an infinite medium have been analysed by Kissling and Young (1989).

We show in Figure 4 the transition in flow directions which occur between bilinear and fracture flow in a bounded multiply fractured reservoir. In the upper plot in Figure 4 the block flows are approximately normal to the fractures, whereas in the lower plot the block flows have changed to being approximately parallel to the fractures. Note that Figure 4 plots the

pressure contours, and the corresponding flow directions are normal to these contours. An analogous effect was reported for the temperature profile in a fractured porous medium (Bodvarson and Tsang 1982).

Pressure drop (bars) at 1.4 seconds



Pressure drop (bars) at 140 seconds

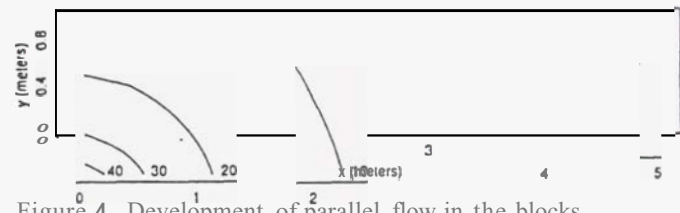


Figure 4. Development of parallel flow in the blocks.

Figure 4 have been drawn assuming  $\epsilon = .1$ ,  $W = 5$ , and  $L = 15$ . This ensures that the bilinear regime develops, before the fracture pressure has effectively travelled along the fracture length, since  $2L \gg \sqrt{\epsilon}$ . It also ensures that parallel flow begins before the width of the block influences pressures, since  $\epsilon/4 \ll 1/9\epsilon \ll W^2/4\epsilon$ . The upper and lower plots in Figure 4 correspond to nondimensional times  $T$  of .1 and 10, respectively.

Since parallel flow in a Cartesian geometry is one dimensional, it is analogous to the initial fracture flow regime, except that now the one dimensional flow occurs in both fracture and block; and both fracture and block have essentially the same pressure gradient. The corresponding pressure regime is then approximated by (14), but with the fracture permeability  $k_f$  replaced by the system average of  $(\delta k_f + w k_b)/(\delta + w)$ , which follows from considering the relationship between mass flow and pressure gradient.

## 4 CONCLUSIONS

This paper has analysed the typical horizontal flow regimes which are likely to occur in finite fractured porous media. The sequence of regimes is not universal, but problem dependent. Some of the mechanisms which alter one regime to another include the interaction of the evolving pressure profiles with the reservoir boundaries, quasi-steady flows formed when fractures and blocks interact strongly, and geometry effects caused when pressure gradients in the fractures are transmitted to the blocks. Figure 1 showed four typical flow regimes: fracture flow; bilinear flow with slope halving; finite block flow with flow doubling; and linear flow with slope doubling.

The non-uniqueness of the flow regimes is indicated in Figure 2, which shows some of the possible scenarios for regime evolution. Four different possibilities are identified in Figure 2, which is constructed by considering constant rates of withdrawal from a well intersecting a single fracture. All possible regime sequences begin with fracture flow, and the governing

## References

pressure equation is (22). Here pressures decrease approximately as  $\sqrt{t}$ , and the withdrawn fluid originates only from the fracture.

A possible later regime is bilinear flow, in which pressure decreases as  $t^{1/4}$ . Here the flow to the well in the fracture results largely from fluid initially in the blocks. These bilinear flows develop if pressures have not propagated to the end of the fracture. The governing equation is quasi-steady, and given in (23). An extensive analysis of bilinear flow has been completed recently (Weir, 1995).

A later regime involves parallel flow, which occurs when significant pressure gradients in the fractures are transmitted to the blocks. Then significant flows occur in the blocks parallel to the fractures, and not normal to them, as for the bilinear regime. (For three dimensional flows, parallel flows is replaced by radial flows.) The parallel regime occurs only in more than one dimension. A typical transition between bilinear flow and parallel flow was given in Figure 4, which also indicates that, away from the sink, it is possible for the majority of the flow to the sink to occur in the blocks.

If the pressure disturbance reaches the end of the fracture before bilinear flow develops, then the finite fracture regime begins. This involves production from decompression of fluid in the fracture alone. It is similar to the final regime of linear flow, but is based on the fracture volume. There will then follow another regime, before the final regime of linear flows begins. The characteristic slope doubling of the finite fracture regime was demonstrated in Figure 3.

We also discussed the finite block regime, but argued that this will usually be replaced by the parallel regime. The finite block regime assumed anisotropic flow in the blocks towards the fractures.

The final regime is the linear drawdown regime, corresponding to the fractures and blocks acting as a lumped storage model. Pressures decrease linearly with time. The development of this regime can be greatly delayed relative to the "expected" times of  $l^2/D_f$  and  $w^2/D_b$ , because of the intermediate regimes.

In addition to the characteristic pressure decreases associated with each regime, we also gave estimates for the times that each regime began and ended. Figures 1 and 3 indicated the accuracy of some of the pressure estimates, and of the beginning and ending times for the regimes.

## 5 ACKNOWLEDGEMENTS

Figure 4 was computed by Dr Stephen White.

- Allis R.G. and Hunt, T.M., 1986, Analysis of Exploitation-Induced Gravity Changes at Wairakei Geothermal Field *Geophysics* **51**(8) 1647-1660.
- Anzelius, A., 1926, Über Erwärmung vermittelt durch-stromender Medien *Zeit. Ang. Math. Mech.* **6** 291 - 294.
- Barenblatt, G.I., Zheltov, I.P. and Kochina, I.N., 1960, Basic concepts in the theory of seepage of homogeneous liquids in fissured rocks *J. Appl. Math. and Mech.* **24** 1286 - 1303.
- Bodvarsson, G.S. and Tsang, C.F., 1982, Injection and thermal breakthrough in fractured geothermal reservoirs *J. Geophys. Res.* **87** (B2) 1031 - 1048.
- Burnell, J.G., Weir, G.J. and Young, R.M., 1991, Self Similar Radial Two Phase Flows *TIPM* **6** 359 - 390.
- Carslaw, H.S. and Jaeger, J.C., 1978 *Conduction of heat in solids* Clarendon Press, Oxford.
- Corey, A.T., 1977 *Mechanics of Heterogeneous Fluids in porous media* Water Resources Publications Fort Collins.
- Earlougher, R. C. , 1977 *Advances in Well Test Analysis* Monograph Volume 5 Henry L. Doherty Series of AIME, Soc. of Petroleum Engineers of AIME, New York.
- Kissling, W. and Young, R.M., 1989, Two-Dimensional Flow in a Fractured Medium *Transport in Porous Media* **4** 335 - 368.
- McGuinness, M., 1986, Pressure Transmission in a Bounded Randomly Fractured Reservoir of Single-Phase Fluid *Transport in Porous Media* **1** 371 - 397.
- Milne, E.A., 1926, The diffusion of imprisoned radiation through a gas *J. London Math. Soc.* **40** - 51.
- Pollard, P. , 1959, Evaluation of Acid Treatments from Pressure Build-Up Analysis *Petroleum Trans. AIME T.P.* **8053** (216) 38 - 43.
- Pruess, K., 1982 *Development of the General Purpose Simulator MULKOM* Report LBL-15500 Lawrence Berkeley Laboratory.
- Pruess, K. , 1988, **SHAFT**, **MULKOM**, **TOUGH** : A set of numerical simulators for multiphase fluid and heat flow *Geothermia, Revistita Mezicana de Geoenergia* **185** -202.
- Warren, J.E. and Root, P.J. , 1963, The behaviour of naturally fractured reservoirs *S.P.E.J.* , Sept. **245** - 255.
- Weir G.J. , 1995, Flow regimes in a finite fractured single phase porous medium *submitted J. Eng. Maths.* ,
- Young, R., 1992, Pressure transients in a double porosity medium *Water Resour. Res.* **27**(6) 1207 - 1214.